

# Myosteatosi predicts survival after surgery for periampullary cancer:

## Citation for published version (APA):

van Dijk, D. P. J., Bakers, F. C. H., Sanduleanu, S., Vaes, R. D. W., Rensen, S. S., Dejong, C. H. C., Beets-Tan, R. G. H., & Damink, S. W. M. O. (2018). Myosteatosi predicts survival after surgery for periampullary cancer: a novel method using MRI. *HPB*, 20(8), 715-720. <https://doi.org/10.1016/j.hpb.2018.02.378>

## Document status and date:

Published: 01/08/2018

## DOI:

[10.1016/j.hpb.2018.02.378](https://doi.org/10.1016/j.hpb.2018.02.378)

## Document Version:

Publisher's PDF, also known as Version of record

## Document license:

Taverne

## Please check the document version of this publication:

- A submitted manuscript is the version of the article upon submission and before peer-review. There can be important differences between the submitted version and the official published version of record. People interested in the research are advised to contact the author for the final version of the publication, or visit the DOI to the publisher's website.
- The final author version and the galley proof are versions of the publication after peer review.
- The final published version features the final layout of the paper including the volume, issue and page numbers.

[Link to publication](#)

## General rights

Copyright and moral rights for the publications made accessible in the public portal are retained by the authors and/or other copyright owners and it is a condition of accessing publications that users recognise and abide by the legal requirements associated with these rights.

- Users may download and print one copy of any publication from the public portal for the purpose of private study or research.
- You may not further distribute the material or use it for any profit-making activity or commercial gain
- You may freely distribute the URL identifying the publication in the public portal.

If the publication is distributed under the terms of Article 25fa of the Dutch Copyright Act, indicated by the "Taverne" license above, please follow below link for the End User Agreement:

[www.umlib.nl/taverne-license](http://www.umlib.nl/taverne-license)

## Take down policy

If you believe that this document breaches copyright please contact us at:

[repository@maastrichtuniversity.nl](mailto:repository@maastrichtuniversity.nl)

providing details and we will investigate your claim.

ORIGINAL ARTICLE

# Myosteatosi predicts survival after surgery for periampullary cancer: a novel method using MRI

David P.J. van Dijk<sup>1,2</sup>, Frans C.H. Bakers<sup>3</sup>, Sebastian Sanduleanu<sup>3</sup>, Rianne D.W. Vaes<sup>1,2</sup>, Sander S. Rensen<sup>1,2</sup>, Cornelis H.C. Dejong<sup>1,2,4,5</sup>, Regina G.H. Beets-Tan<sup>5,6</sup> & Steven W.M. Olde Damink<sup>1,2,4</sup>

<sup>1</sup>Department of Surgery, Maastricht University Medical Centre, Maastricht, <sup>2</sup>NUTRIM School of Nutrition and Translational Research in Metabolism, Maastricht University, <sup>3</sup>Department of Radiology and Nuclear Medicine, Maastricht University Medical Centre, Maastricht, The Netherlands, <sup>4</sup>Department of General, Visceral and Transplantation Surgery, RWTH University Hospital Aachen, Aachen, Germany, <sup>5</sup>GROW School for Oncology and Developmental Biology, Maastricht University, Maastricht, and <sup>6</sup>Department of Radiology, Netherlands Cancer Institute-Antoni van Leeuwenhoek, Amsterdam, The Netherlands

## Abstract

**Background:** Myosteatosi, characterized by inter- and intramyocellular fat deposition, is strongly related to poor overall survival after surgery for periampullary cancer. It is commonly assessed by calculating the muscle radiation attenuation on computed tomography (CT) scans. However, since magnetic resonance imaging (MRI) is replacing CT in routine diagnostic work-up, developing methods based on MRI is important. We developed a new method using MRI-muscle signal intensity to assess myosteatosi and compared it with CT-muscle radiation attenuation.

**Methods:** Patients were selected from a prospective cohort of 236 surgical patients with periampullary cancer. The MRI-muscle signal intensity and CT-muscle radiation attenuation were assessed at the level of the third lumbar vertebra and related to survival.

**Results:** Forty-seven patients were included in the study. Inter-observer variability for MRI assessment was low ( $R^2 = 0.94$ ). MRI-muscle signal intensity was associated with short survival: median survival 9.8 (95%-CI: 1.5–18.1) vs. 18.2 (95%-CI: 10.7–25.8) months for high vs. low intensity, respectively ( $p = 0.038$ ). Similar results were found for CT-muscle radiation attenuation (low vs. high radiation attenuation: 10.8 (95%-CI: 8.5–13.1) vs. 15.9 (95%-CI: 10.2–21.7) months, respectively;  $p = 0.046$ ). MRI-signal intensity correlated negatively with CT-radiation attenuation ( $r = -0.614$ ,  $p < 0.001$ ).

**Conclusions:** Myosteatosi may be adequately assessed using either MRI-muscle signal intensity or CT-muscle radiation attenuation.

Received 18 September 2017; accepted 4 February 2018

## Correspondence

David P.J. van Dijk, Universiteitssingel 50, 6229 ER, Maastricht, The Netherlands. E-mail: [d.vandijk@maastrichtuniversity.nl](mailto:d.vandijk@maastrichtuniversity.nl)

## Background

The use of single slice computed tomography (CT) imaging for risk assessment has become increasingly popular for various types of diseases.<sup>1,2</sup> A single CT-slide can be used to estimate total body amounts of skeletal muscle, visceral adipose tissue, and subcutaneous adipose tissue.<sup>3</sup> Next to body-composition, CT-scans provide additional information, such as the muscle

radiation attenuation or muscle radio density: the average Hounsfield unit value of the skeletal muscle tissue at the L3 level.<sup>4</sup> Low muscle radiation attenuation is a sign of myosteatosi, a condition associated with poor survival in various types of cancer.<sup>1</sup> We previously found a strong association between myosteatosi and overall survival in multivariate analysis in patients with periampullary cancer.<sup>5</sup> Myosteatosi has been associated with a systemic inflammatory response in cancer patients,<sup>6,7</sup> which could be related to cancer cachexia, a syndrome of severe weight loss and muscle wasting.<sup>8</sup> The possible

**Funding:** This work was partly funded by the Netherlands Organization for Scientific Research (NWO Grant 022.003.011).

link with cancer cachexia might be an explanation for the strong survival effect of myosteatosis. Although mostly CT-scans are used for assessment of myosteatosis, magnetic resonance imaging (MRI) provides higher contrast for soft tissue and could therefore be superior to CT for visualizing soft tissue such as skeletal muscle. However, to our knowledge there are no studies assessing myosteatosis using MRI-scans. Developing MRI-based methods is important since MRI-scans are increasingly used in routine diagnostic work-up and follow-up of (periampullary) cancer, sometimes even replacing CT-scans.<sup>9,10</sup> In this study, we compared MRI muscle signal intensity with CT muscle radiation attenuation as markers of myosteatosis and assessed the association of both markers with overall survival in patients with periampullary cancer undergoing pancreatic surgery.

## Methods

### Subjects

A prospective cohort of 236 patients undergoing pancreatic surgery between 2008 and 2014 at the Maastricht University Medical Centre (MUMC), the Netherlands was studied. From this cohort, one hundred and eighty-six patients have been reported on before in the context of the relationship between myosteatosis and overall survival using CT imaging alone.<sup>5</sup> Patients were included for analysis if they had pathology-proven or radiology-proven periampullary cancer and both a preoperative CT-scan and MRI-scan available (<2 months before surgery). Exclusion criteria were the presence of a neuro-endocrine tumor, benign disease, or pre-malignant disease (such as intraductal papillary mucinous neoplasm).

### Data collection

The primary outcome parameter of this study was overall survival, measured in months from the day of surgery. Secondary outcome was the correlation between CT muscle radiation attenuation in HUs and MRI muscle signal intensity. Patient-reported weight, height, and weight loss in the six months prior to surgery as well as age and sex were recorded at the outpatient department. Comorbidities (diabetes mellitus, cardiac, pulmonary, and/or renal disorders) were retrieved from the patient's medical file. The most important severe post-operative complications, which are included in the pancreaticoduodenectomy composite endpoint (Dindo-Clavien grade  $\geq 3$ ),<sup>11</sup> were recorded postoperatively until 90 days after surgery. These included intra-abdominal abscess, sepsis, gastrojejunostomy leakage, post-pancreaticoduodenectomy hemorrhage, bile leakage/hepaticojejunostomy leakage, pancreatic fistula/pancreatic anastomosis leakage, delayed gastric emptying, and mortality. Definitive diagnosis and tumor staging were based on the pathology report of the resected specimen. The study protocol was approved by the medical ethical committee of the MUMC which waived the requirement to obtain informed consent.

### Image analysis

Abdominal CT-scans and MRI-scans were analyzed in anonymized format. Two blinded researchers trained in radiologic anatomy and body composition analysis (DvD and FB) evaluated the MRI-scans independently. CT-scans were evaluated by DvD alone, as CT-body composition analysis has been validated before.<sup>1,3</sup> First, a single slice of each patient's CT-scan and MRI-scan was selected at the level of the third lumbar vertebra (L3). For MRI-scans, only T2 weighted images were selected. When multiple slices at L3 were available, the slice on which both transverse processes were best visible was selected. CT-scans and MRI-scans were all screened before analysis by an abdominal radiologist for poor quality and large radiation artifacts, or if parts of muscle tissue were not visualized on the dorsal or both lateral edges. These scans were excluded from analysis. Since many MRI-scans suffered from radiological artifacts on the ventral side, only the dorsal portion of the muscles (at the ventral border of the body of the L3 vertebra) was analyzed for both CT and MRI-scans (see Fig. 1). Scans were analyzed using sliceOmatic 5. (TomoVision, Magog, Canada) software for Microsoft Windows®. Myosteatosis was defined as a low CT muscle radiation attenuation or a high MRI muscle signal intensity. For CT-images, the cross-sectional area (cm<sup>2</sup>) of the dorsal skeletal muscles was measured including intermuscular adipose tissue (IMAT). The muscle radiation attenuation was assessed by calculating the average HU value of the total muscle area. The same was done for MRI-images, but instead of average HU value, the average signal intensity of the total muscle area was calculated. Since signal intensity is scaled per acquired sequence, the measured intensity cannot be compared within or between patients, making normalization against an internal standard necessary. Therefore, we normalized muscle signal intensity using the cerebrospinal fluid signal (CSF) intensity. The rationale behind this approach is based on the similarity of the signal intensity of CSF and water, the availability of CSF within L3 slides, and the assumed stable relation between muscle and CSF signal intensity within a single patient. Normalization with CSF signal intensity had therefore high potential to correct for signal intensity differences among different scan sessions and patients. Cerebrospinal fluid signal intensity was calculated for the total visible area of CSF (excluding any nervous tissue) at the same level as the skeletal muscle assessment (L3). The average values of the two observers' MRI measurements were used for analysis.

### Statistical analysis

Since there are no published cut-offs for MRI muscle signal intensity and our cohort was too small for cut point analysis by optimal stratification,<sup>12</sup> we determined sex-specific cut-off values based on tertiles, which is a common method for small cohorts.<sup>5,13</sup> Cut-off values were set at the lowest tertile for muscle radiation attenuation and at the highest tertile for MRI muscle signal intensity. Data were analyzed using IBM SPSS 23 for Microsoft Windows®. Inter-observer variability was assessed

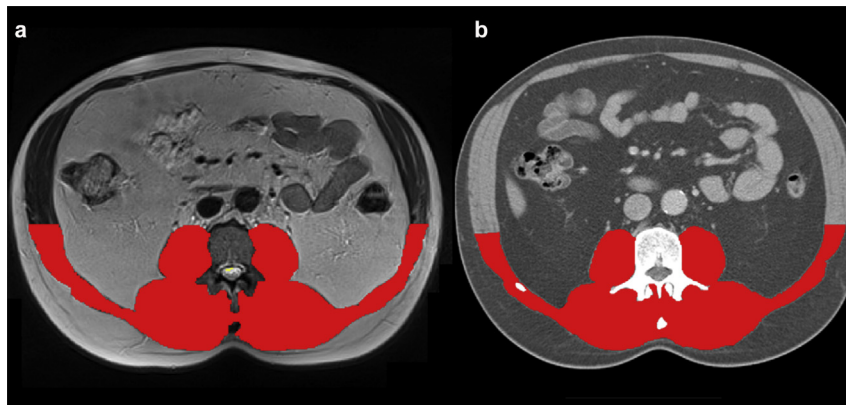


**Figure 1** MRI (a) and CT (b) annotations for skeletal muscle analysis. The dorsal portion of total muscle tissue was annotated at L3 level (red). For MRI (a), the average signal intensity was calculated and corrected for cerebrospinal fluid signal intensity. For CT (b), the average Hounsfield units value was calculated (radiation attenuation). CT = computed tomography, MRI = magnetic resonance imaging

using linear regression and by calculating the root mean square of coefficients of variation. Cohen's kappa ( $\kappa$ ) was used to indicate the inter-observer agreement of high vs. low MRI muscle signal intensity. The Kaplan Meier estimate was used to assess the association of muscle radiation attenuation and muscle signal intensity with survival. The reverse Kaplan–Meier estimate was used to estimate the median follow-up time. For correlation, Pearson's correlation coefficient ( $r$ ) was used. A  $p$ -value of  $<0.05$  was considered significant.

## Results

### Patient cohort

From all 236 patients of the prospective cohort, 55 patients had both a CT-scan and MRI-scan available. Eight patients were excluded because of IPMN ( $n = 4$ ) or benign disease ( $n = 4$ ), resulting in a final number of 47 patients included into this study. Median follow-up was 59.8 months. Patient characteristics are shown in [Table 1](#).

### Image analysis

After scoring for quality, two CT-scans and two MRI-scans were scored as poor and therefore excluded from the analysis. The inter-observer variability of the MRI assessments was low ( $R^2 = 0.94$ , root mean square of coefficients of variation = 4.4%; see [Fig. 2](#)). Mean and sex-specific cut-offs are given in [Table 2](#). Myosteatosis was defined as a muscle radiation attenuation of  $<27.0$  HU (males) and  $<17.5$  HU (females) or as a corrected MRI muscle signal intensity of  $>0.33$  (males) and  $>0.36$  (females). Inter-observer agreement was high ( $\kappa = 0.90$ ,  $p < 0.001$ ). There were no significant differences in patient characteristics between patients with low vs. moderate-high CT radiation attenuation or between patients with high vs moderate-low MRI signal intensity ( $p > 0.05$  for all characteristics listed in [Table 1](#)). Without correction for CSF signal intensity, MRI muscle signal intensity did not correlate with CT muscle radiation attenuation

**Table 1** Patient characteristics

	Patients (n = 47)
Age (years)	67.4 ± 10.7
Male (n, %)	24 (51.1%)
BMI (kg/m <sup>2</sup> )	24.8 ± 4.1
Pathology (n, %)	
Pancreatic	19 (40.4%)
Ampullary	12 (25.5%)
Cholangiocarcinoma	4 (8.5%)
Other	2 (4.2%)
None available (palliative surgery)	10 (21.3%)
Comorbidity (n, %)	
Diabetes mellitus	10 (21.3%)
Cardiac	17 (36.3%)
Pulmonary	5 (10.6%)
Renal	2 (4.3%)
Postoperative complications <sup>a</sup> (n, %)	19 (40.4%)

Patient characteristics of the study cohort. Continuous variables are shown as mean ± standard deviation.

<sup>a</sup>Patients had one or more of the following complications: Intra-abdominal abscess, sepsis, gastrojejunostomy leakage, post-pancreaticoduodenectomy hemorrhage, bile leakage, pancreatic fistula, delayed gastric emptying, or operative mortality (within 90 days after surgery).

( $r = -0.055$ ,  $p = 0.727$ ). After correction for CSF signal intensity, MRI muscle signal intensity was inversely correlated with CT muscle radiation attenuation ( $r = -0.614$ ,  $p < 0.001$ ; see [Fig. 3](#)).

### Survival analysis

Survival analysis was performed for CT and MRI assessments separately using the Kaplan–Meier estimate. Patients with low CT muscle radiation attenuation had a lower survival than patients with moderate to high radiation attenuation: median

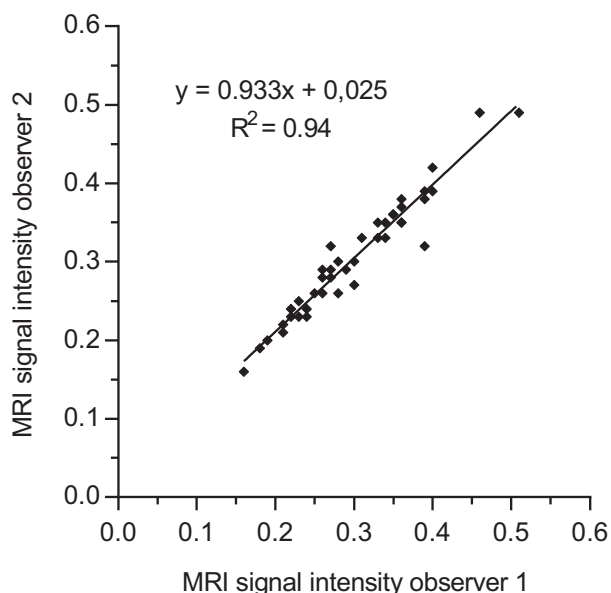


**Figure 2** Inter-observer variability of MRI muscle signal intensity. MRI muscle signal intensity inter-observer variability was low ( $R^2 = 0.94$ , root mean square of coefficients of variation = 4.4%) MRI muscle signal intensity was corrected for cerebrospinal fluid signal intensity. MRI = magnetic resonance imaging

survival 10.8 (95%-CI: 8.5–13.1) vs. 15.9 (95%-CI: 10.2–21.7) months, respectively ( $p = 0.046$ ; see Fig. 4). Patients with high MRI muscle signal intensity had lower survival than patients with moderate to low signal intensity: median survival 9.8 (95%-CI: 1.5–18.1) vs. 18.2 (95%-CI: 10.7–25.8) months, respectively ( $p = 0.038$ ; see Fig. 4).

## Discussion

This study demonstrates that myosteatosis, reflected by either low CT muscle radiation attenuation or high MRI muscle signal intensity, is associated with reduced survival in patients with periampullary cancer. This is the first study describing a method to quantify myosteatosis using MRI scans. Myosteatosis is an important predictor of overall survival in patients with periampullary cancer<sup>5,6,14</sup> and other cancers.<sup>1</sup> Also, in benign disease such as liver cirrhosis, myosteatosis has been associated with

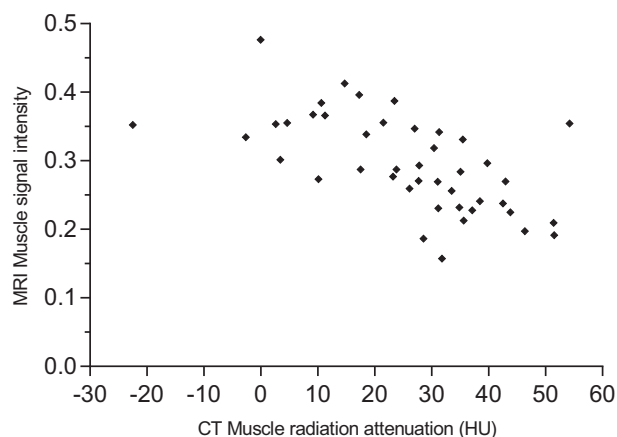


**Figure 3** Correlation between CT muscle radiation attenuation and MRI muscle signal intensity. CT muscle radiation attenuation was inversely correlated with MRI muscle signal intensity ( $r = -0.614$ ,  $p < 0.001$ ). MRI muscle signal intensity was corrected for cerebrospinal fluid signal intensity. CT = computed tomography, MRI = magnetic resonance imaging

poor survival.<sup>2</sup> Developing MRI-based methods to assess muscle mass and fat content is important since MRI-scans increasingly replace CT-scans in the diagnostic work-up of various malignancies. Moreover, many benign diseases only use MRI-scans for diagnosis or follow-up (e.g. inflammatory bowel disease).

Shen et al. previously showed that MRI based measurements of skeletal muscle mass correlated well with CT-based measurements of skeletal muscle mass.<sup>15</sup> In the present study, we demonstrate that MRI muscle signal intensity should be normalized using CSF signal intensity to achieve an acceptable correlation with CT-scan muscle radiation attenuation. The few previous MRI based studies on myosteatosis only assessed IMAT,<sup>16–23</sup> which is visible adipose tissue in between the muscle tissue rather than steatosis of the muscle tissue itself.<sup>4</sup> Methods assessing IMAT area vary greatly among studies: some studies only measure anatomically visible IMAT area,<sup>16,17</sup> while others identify all tissue with a MRI signal intensity 20% lower than the subcutaneous adipose tissue signal intensity as IMAT.<sup>18,19</sup> Although these methods could be adequate for rough IMAT estimations, the cut-offs used for IMAT delineation are arbitrary. Subcutaneous adipose tissue signal intensity is affected by its

**Table 2** Mean sex-specific cut-off values for CT muscle radiation attenuation and MRI muscle signal intensity

	Male (n = 24)		Female (n = 23)		Total (n = 47)
	Mean (SD)	Cut-off	Mean (SD)	Cut-off	Mean (SD)
Muscle radiation attenuation (HU)	27.0 (18.7)	27.0	23.3 (13.7)	17.5	25.2 (16.3)
Muscle signal intensity	0.28 (0.08)	0.33	0.32 (0.07)	0.36	0.30 (0.07)

Sex-specific cut-offs were made at the lower tertile for radiation attenuation and at the higher tertile for MRI signal intensity, which both are considered to reflect ectopic fat accumulation in muscle tissue. Four scans (two CT-scans and two MRI-scans) were not included because of poor quality. MRI muscle signal intensity was corrected for cerebrospinal fluid signal intensity.

CT = computed tomography, HU = Hounsfield unit, MRI = magnetic resonance imaging, SD = standard deviation.

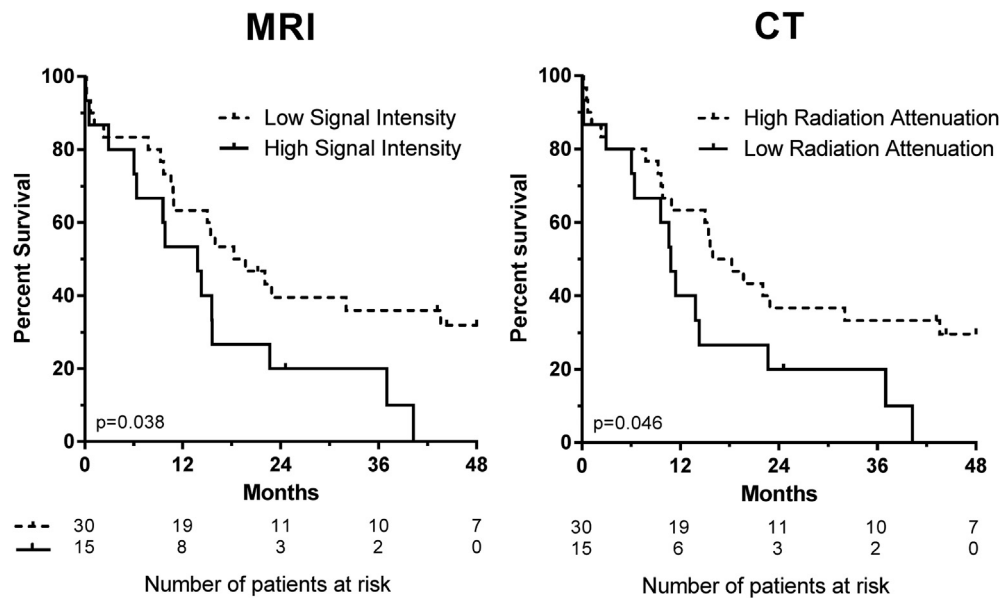


**Figure 4** Association between overall survival and high MRI muscle signal intensity/low CT muscle radiation attenuation. MRI muscle signal intensity and low CT muscle radiation attenuation showed a similar negative association with survival. MRI muscle signal intensity was corrected for cerebrospinal fluid signal intensity. CT = computed tomography, MRI = magnetic resonance imaging

triglyceride content and therefore not a stable internal correction factor. Some studies choose for a more objective approach by producing histograms and dividing the tissue into areas with high (IMAT) and low (muscle) signal intensity,<sup>20</sup> mostly by automatic segmentation.<sup>21–23</sup> However, IMAT distribution is highly heterogeneous among different muscles and slices. While single L3 slice estimations of skeletal muscle, visceral adipose tissue, and subcutaneous adipose tissue correlate well with total body volumes,<sup>24</sup> IMAT does not.<sup>25</sup> Therefore, IMAT should be assessed using total body scans instead of single L3 slices.<sup>25</sup>

In the present study, we assessed myosteatosis as an increase of intramyocellular lipid content rather than increased IMAT in between the muscle tissue. Stephens et al. previously showed that the amount and size of intramyocellular lipid droplets were inversely correlated with CT muscle radiation attenuation.<sup>26</sup> Moreover, the amount of intramyocellular lipid droplets increased with progression of cachexia. We therefore recommend assessing indices of muscle lipid content rather than IMAT as markers of myosteatosis.

There are some limitations to this study. The MRI images used were targeted towards diagnosis of periampullary cancer rather than muscle analysis. Since this is the first report validating MRI for assessing myosteatosis, the ideal scan settings should be the focus of future research. Also, IMAT was included in the signal intensity assessments. Ideally, IMAT should be excluded from muscle analysis because of its heterogeneous distribution, as described above. A combination of muscle signal intensity assessment and internal correction by CSF signal intensity as well as automatic segmentation to exclude IMAT would be the best way forward. Unfortunately, our study

did not include the gold standard muscle biopsy-based method to assess performance statistics for CT and MRI. The moderate to strong correlation between CT and MRI assessment of myosteatosis suggests that both image modalities do not necessarily replace each other. A larger study including a gold standard method (e.g. triglyceride measurement on muscle biopsies) should be conducted to prove the (external) validity of measurements performed on CT and MRI studies. Lastly, our study cohort was too small for multivariate analysis. However, we previously demonstrated the association between CT-based myosteatosis and overall survival using multivariate cox-regression analysis.<sup>5</sup>

In conclusion, myosteatosis may be adequately assessed using either CT muscle radiation attenuation or MRI muscle signal intensity. MRI muscle signal intensity should be corrected for CSF signal intensity as an internal standard. There was a strong relationship between both CT- and MRI-based assessments of myosteatosis and postoperative survival of patients with periampullary cancer. This novel MRI-based method can be useful for risk assessment in patients without an available CT-scan, and its use should be explored in risk assessment for diseases in which exclusively MRI-scans are used in the diagnostic workup.

#### Acknowledgement

We would like to thank Jos Slenter for his help in retrieving the radiology images.

#### Funding and conflict of interest

David van Dijk is supported as a PhD-candidate by the Netherlands Organization for Scientific Research (NWO Grant 022.003.011).

All authors declare that they have no conflict of interest.

## References

1. Martin L, Birdsall L, Macdonald N, Reiman T, Clandinin MT, McCargar LJ *et al.* (2013) Cancer cachexia in the age of obesity: skeletal muscle depletion is a powerful prognostic factor, independent of body mass index. *J Clin Oncol* 31:1539–1547.
2. Montano-Loza AJ, Angulo P, Meza-Junco J, Prado CMM, Sawyer MB, Beaumont C *et al.* (2016) Sarcopenic obesity and myosteatosis are associated with higher mortality in patients with cirrhosis. *J Cachexia Sarcopenia Muscle* 7:126–135.
3. Mourtzakis M, Prado CMM, Lieffers JR, Reiman T, McCargar LJ, Baracos VE. (2008) A practical and precise approach to quantification of body composition in cancer patients using computed tomography images acquired during routine care. *Appl Physiol Nutr Metab* 33: 997–1006.
4. Aubrey J, Esfandiari N, Baracos VE, Buteau FA, Frenette J, Putman CT *et al.* (2014) Measurement of skeletal muscle radiation attenuation and basis of its biological variation. *Acta Physiol (Oxf)* 210:489–497.
5. van Dijk DP, Bakens MJ, Coolsen MMM, Rensen SS, van Dam RM, Bours MJ *et al.* (2017) Low skeletal muscle radiation attenuation and visceral adiposity are associated with overall survival and surgical site infections in patients with pancreatic cancer. *J Cachexia Sarcopenia Muscle* 8:317–326.
6. Rollins KE, Tewari N, Ackner A, Awwad A, Madhusudan S, Macdonald IA *et al.* (2015) The impact of sarcopenia and myosteatosis on outcomes of unresectable pancreatic cancer or distal cholangiocarcinoma. *Clin Nutr (Edinburgh, Scotland)* 35:1103–1109.
7. Malietzis G, Johns N, Al-Hassi HO, Knight SC, Kennedy RH, Fearon KC *et al.* (2015) Low muscularity and myosteatosis is related to the host systemic inflammatory response in patients undergoing surgery for colorectal cancer. *Ann Surg* 263:320–325.
8. Fearon K, Strasser F, Anker SD, Bosaeus I, Bruera E, Fainsinger RL *et al.* (2011) Definition and classification of cancer cachexia: an international consensus. *Lancet Oncol* 12:489–495.
9. Zhang Q, Chen S, Zeng L, Chen Y, Lian G, Qian C *et al.* (2017) New developments in the early diagnosis of pancreatic cancer. *Expert Rev Gastroenterol Hepatol* 11:149–156.
10. Nerad E, Lambregts DM, Kersten EL, Maas M, Bakers FC, van den Bosch HC *et al.* (2017) MRI for local staging of colon cancer: can MRI become the optimal staging modality for patients with colon cancer? *Dis Colon Rectum* 60:385–392.
11. Coolsen MM, Clermonts SH, van Dam RM, Winkens B, Malagó M, Fusai GK *et al.* (2013) Development of a composite endpoint for randomized controlled trials in pancreaticoduodenectomy. *World J Surg* 38:1468–1475.
12. Williams BA, Mandrekar JN, Mandrekar SJ, Cha SS, Furth AF. (2006) *Finding optimal cutpoints for continuous covariates with binary and time-to-event outcomes*. Rochester, MN: Mayo Foundation.
13. Martin L. (2016) Diagnostic criteria for cancer cachexia: data versus dogma. *Curr Opin Clin Nutr Metab Care* 19:188–198.
14. Okumura S, Kaido T, Hamaguchi Y, Fujimoto Y, Masui T, Mizumoto M *et al.* (2015) Impact of preoperative quality as well as quantity of skeletal muscle on survival after resection of pancreatic cancer. *Surgery* 157: 1088–1098.
15. Shen W, Punyanitya M, Wang Z, Gallagher D, St-Onge M-PP, Albu J *et al.* (2004) Total body skeletal muscle and adipose tissue volumes: estimation from a single abdominal cross-sectional image. *J Appl Physiol (Bethesda, Md: 1985)* 97:2333–2338.
16. Hu Z-JJ, He J, Zhao F-DD, Fang X-QQ, Zhou L-NN, Fan S-WW. (2011) An assessment of the intra- and inter-reliability of the lumbar paraspinal muscle parameters using CT scan and magnetic resonance imaging. *Spine* 36:74.
17. Zoico E, Rossi A, Di Francesco V, Sepe A, Oliosio D, Pizzini F *et al.* (2010) Adipose tissue infiltration in skeletal muscle of healthy elderly men: relationships with body composition, insulin resistance, and inflammation at the systemic and tissue level. *J Gerontol Ser A Biol Sci Med Sci* 65:295–299.
18. Song M-YY, Ruts E, Kim J, Janumala I, Heymsfield S, Gallagher D. (2004) Sarcopenia and increased adipose tissue infiltration of muscle in elderly African American women. *Am J Clin Nutr* 79:874–880.
19. Rossi A, Zoico E, Goodpaster BH, Sepe A, Di Francesco V, Fantin F *et al.* (2010) Quantification of intermuscular adipose tissue in the erector spinae muscle by MRI: agreement with histological evaluation. *Obesity (Silver Spring, Md)* 18:2379–2384.
20. D'Hooge R, Cagnie B, Crombez G, Vanderstraeten G, Dolphens M, Danneels L. (2012) Increased intramuscular fatty infiltration without differences in lumbar muscle cross-sectional area during remission of unilateral recurrent low back pain. *Man Ther* 17:584–588.
21. Gorgey AS, Dudley GA. (2007) Skeletal muscle atrophy and increased intramuscular fat after incomplete spinal cord injury. *Spinal Cord* 45: 304–309.
22. Positano V, Cusi K, Santarelli MF, Sironi A, Petz R, Defronzo R *et al.* (2008) Automatic correction of intensity inhomogeneities improves unsupervised assessment of abdominal fat by MRI. *J Magn Reson Imaging JMRI* 28:403–410.
23. Positano V, Christiansen T, Santarelli MF, Ringgaard S, Landini L, Gastaldelli A. (2009) Accurate segmentation of subcutaneous and intermuscular adipose tissue from MR images of the thigh. *J Magn Reson Imaging JMRI* 29:677–684.
24. Schweitzer L, Geisler C, Pourhassan M, Braun W, Glüer C-CC, Bösych Westphal A *et al.* (2015) What is the best reference site for a single MRI slice to assess whole-body skeletal muscle and adipose tissue volumes in healthy adults? *Am J Clin Nutr* 102:58–65.
25. Ruan X, Gallagher D, Harris T, Albu J, Heymsfield S, Kuznia P *et al.* (2007) Estimating whole body intermuscular adipose tissue from single cross-sectional magnetic resonance images. *J Appl Physiol* 102: 748–754.
26. Stephens NA, Skipworth RJE, MacDonald AJ, Greig CA, Ross JA, Fearon KCH. (2011) Intramyocellular lipid droplets increase with progression of cachexia in cancer patients. *J Cachexia Sarcopenia Muscle* 2:111–117.